

Supporting Information for

Insights into overall photocatalytic water splitting through simultaneous *in situ* H₂ and O₂ measurements

Nadzeya Brezhneva, Alexander Eith, Ebrahim Abedini, Daniel Kowalczyk, Dirk Ziegenbalg, Jacob Schneidewind

Corresponding author(s), e-mail: jacob.schneidewind@uni-jena.de

Other supplementary materials for this manuscript:

Original data, analysis code and kinetic model code are publicly available at:

Github: https://github.com/water-splitting-group/o2_h2_reactor and

https://github.com/jschneidewind/simultaneous_detection

1. Table of contents

1. Table of contents.....	2
1.1. List of figures.....	3
1.2. List of tables.....	4
2. Experimental information.....	5
2.1. Reagents and equipment.....	5
3. Photocatalyst preparation and characterization.....	7
3.1. Calcination of SrCO ₃	7
3.2. Preparation of SrTiO ₃	7
3.3. Al doping of SrTiO ₃	8
3.4. RhCl ₃ ×3H ₂ O and Cr(NO ₃) ₃ ×9H ₂ O stock solutions preparation.....	9
3.5. Loading of Al:SrTiO ₃ with Rh _{2-y} Cr _y O ₃ co-catalyst.....	9
3.6. Photocatalyst characterization.....	10
4. Photocatalytic experiment hardware.....	12
4.1. Irradiation setup and chamber.....	12
4.2. Irradiation reactor.....	13
4.3. Irradiance determination chamber.....	14
4.4. Experimental setup for measurements in liquid and gas phase.....	15
5. Photocatalytic experiments with O₂ and H₂ simultaneous detection.....	16
5.1. Photocatalyst suspension preparation.....	16
5.2. Main steps in photocatalytic tests.....	16
6. Overview of performed photocatalytic tests.....	17
7. Analytical data.....	19
7.1. Spectrum of light source.....	19
8. Data processing and analysis.....	20
8.1. Detailed description of data processing workflow.....	20
8.2. Liquid/gas phase mass transport during photocatalytic water splitting.....	20
8.3. Processed experimental data.....	22
8.4. Arrhenius analysis of temperature dependent data.....	26
9. References.....	26

1.1. List of figures

- [Figure 1: SEM images of Al:SrTiO₃ loaded with Rh_{2-y}Cr_yO₃ co-catalyst at different magnifications](#)
- [Figure 2: Spectral distribution of the main elements in Al:SrTiO₃ loaded with Rh_{2-y}Cr_yO₃ photocatalyst \(top\), EDX overview of the sample \(bottom\)](#)
- [Figure 3: XRD plot of the Al:SrTiO₃ loaded with Rh_{2-y}Cr_yO₃ co-catalyst](#)
- [Figure 4: Irradiation setup with installed reactor and sensors. Left: complete irradiation setup, right: close-up of the irradiation chamber](#)
- [Figure 5: Reactor used for irradiation experiments. Left: Side view with shorter NS14 outlet in front, right: rotated view](#)
- [Figure 6: Important steps during photocatalytic tests: calibration of H₂ sensor under degassed conditions \(left\), degassing of the photocatalyst suspension \(center\), after start of irradiation, top view \(right\)](#)
- [Figure 7: Emission spectrum of 365 nm LED \(provided by Mightex\)](#)
- [Figure 8: Experimental data and kinetic modelling of H₂/O₂ evolution in the liquid \(A\) and gas phase \(B\). For both measurements the evolution of the gases over time is shown \(black and grey dots\) as well as the ratio between the two gases \(right axis, green dots\). The concentration of the liquid phase gases is given in μmol·L⁻¹ and the gas phase concentration is given in an analogous unit of μmol·L⁻¹, which indicates the amount of gases formed per liter of irradiated liquid phase volume \(to have consistent units for the kinetic modelling\). To both the liquid and the gas phase data one kinetic model \(C\) with one set of rate constants is fitted \(black, grey and green lines\). The optimized values for the rate constants are: k₁ = 4.1·10⁻⁹ s⁻¹, k₂ = 2.3·10⁻³ s⁻¹, k₃ = 2.2·10⁻³ s⁻¹, k₄ = 5.8·10⁻³.](#)
- [Figure 9: Experimental data for H₂/O₂ simultaneous measurements \(reference conditions\)](#)
- [Figure 10: Experimental data for H₂/O₂ simultaneous measurements \(screening of irradiance: 20 mW·cm⁻², 100 mW·cm⁻², 150 mW·cm⁻²\)](#)
- [Figure 11: Experimental data for H₂/O₂ simultaneous measurements \(screening of temperature: 10 °C, 30 °C\)](#)
- [Figure 12: Experimental data for H₂/O₂ simultaneous measurements \(screening of co-catalyst loading: 0.0005 wt. fraction Rh/Cr, 0.002 wt. fraction Rh/Cr\)](#)
- [Figure 13: Experimental data for H₂/O₂ simultaneous measurements \(kinetic isotope effect investigation\)](#)
- [Figure 14: Experimental data for H₂/O₂ simultaneous measurements in gas phase \(left: H₂O as a dispersion medium, right: D₂O as a dispersion medium for kinetic isotope effect investigation\)](#)
- [Figure 15: Arrhenius analysis of temperature dependent liquid phase experimental data to determine the thermal activation energy](#)

1.2. List of tables

- [Table 1. Overview of main reagents used for photocatalyst preparation and photocatalytic tests](#)
- [Table 2. Overview of main equipment used for photocatalyst preparation and photocatalytic tests](#)
- [Table 3. List of the equipment used in the photocatalytic tests for O₂ and H₂ measurements in liquid and gas phase](#)
- [Table 4. Overview of main screening parameters](#)
- [Table 5. Classification of performed photocatalytic tests](#)

2. Experimental information

2.1. Reagents and equipment

List of the chemicals used in work is presented in [table 1](#) below:

Table 1. Overview of main reagents used for photocatalyst preparation and photocatalytic tests

Name of the reagent, purity	Supplier
SrCO ₃ , > 98.0%	TCI
TiO ₂ , Aerioxide® P25	Thermo Scientific
SrCl ₂ ×6H ₂ O, 99% (ACS)	Strem Chemicals
AgNO ₃	VEB Feinchemie Sebnitz
RhCl ₃ ×3H ₂ O	BLD Pharmatech GmbH
Cr(NO ₃) ₃ ×9H ₂ O	Acros Organics
Ethanol, 96%	/
D ₂ O, 99.90 %	Eurisotop

In all experiments milli-Q water (18.2 MΩ·cm) was used.

List of the used equipment is provided in [table 2](#) below.

Table 2. Overview of main equipment used for photocatalyst preparation and photocatalytic tests

Name of the step	Model of the device	Supplier
Photocatalyst preparation	Muffle furnace Nabertherm LT 15/11/P330	Nabertherm GmbH
	Muffle furnace Nabertherm L3/11/P320	Nabertherm GmbH
	Drying oven Binder FD 56 E3.1	Binder GmbH
	Ultrasound bath ELMA Fischerbrand Select 30	Fischer Scientific
	Magnetic stirrer Heidolph Instruments Hei-PLATE Mix'n'Heat Core+Ø135	LT Laborhandel GmbH
	Vortex mixer VV3	VWR
Irradiation	Double walled beaker	Glassblower

	Thermostat LAUDA LOOP L 100	LAUDA
	Ultra-high power LED LCS-6500-65-22, 365 nm	Mightex Systems
	Power meter Newport 843-R-USB	Newport Spectra-Physics GmbH
	Thermopile sensor Newport 919P-020-12	Newport Spectra-Physics GmbH
Gas and liquid phase O ₂ detection	Trace range robust probe OXROB10	PyroScience GmbH
	Firesting Fiber-Optic Oxygen Meter 2 Channel	PyroScience GmbH
	PT100 temperature sensor	Therma Thermofühler GmbH
Gas and liquid phase H ₂ detection	H ₂ UniAmp Single Channel system (amplifier)	Unisense
	Normal range hydrogen sensor H ₂ UniAmp Sensor - Normal range - 2.1 x 80 mm needle	Unisense
	PT1000 temperatures sensor	Therma Thermofühler GmbH
Photocatalyst characterization	TESCAN Mira scanning electron microscope	TESCAN
	XRD-BRUKER-D2 PHASER diffractometer	Bruker

Scanning electron microscopy (SEM) of the Al:SrTiO₃ loaded with Rh_{2-y}Cr_yO₃ (0.1 wt% Rh,Cr) photocatalyst was performed using a TESCAN MIRA microscope equipped with a secondary electron detector and operated at an accelerating voltage of 5 kV. The sample powder was mounted on conductive carbon adhesive pads attached to aluminum pin stubs. Energy-dispersive X-ray (EDX) spectroscopy was carried out using an Essence™ EDS system equipped with an integrated detector featuring a 30 mm² active area and a Si₃N₄ window, providing an energy resolution of 129 eV at the Mn K α line.

XRD measurements of the photocatalyst were performed using XRD-BRUKER-D2 PHASER diffractometer.

The measurements were performed with the following parameters:

1. Tube: Cu tube with 1.54184 [Å],
2. Detector: SSD160_2 (1D mode),
3. 2θ start from 5°, stop at 100°, Increment: 0.02°,

4. 1.00 sec per step, 4701 steps, Total time: 4801 sec.
5. Scan type: Coupled 2θ/θ,
6. Scan mode: Continuous PSD fast.
7. Sample holder: Specimen stainless steel silicon ground

3. Photocatalyst preparation and characterization

Preparation of Al:SrTiO₃ loaded with Rh_{2-y}Cr_yO₃ co-catalyst was inspired by the group of Prof. F. Osterloh [1]. Initially, SrTiO₃ was prepared via solid-state synthesis from SrCO₃ and TiO₂ (1000 °C, 10 h), followed by Al-doping procedure in alumina crucibles in the presence of SrCl₂ (1000 °C, 10 h) used as a flux medium. Afterwards, the obtained product was washed with milli-Q water (to remove SrCl₂ till no Cl⁻ could be detected with 0.1 M AgNO₃ solution) and dried at 100 °C overnight. The co-catalyst loading was performed *via* wet impregnation method using RhCl₃×3H₂O and Cr(NO₃)₃×9H₂O solutions to achieve 0.1 wt% Rh and Cr in the final product. The detailed description of each step of material synthesis is provided below.

3.1. Calcination of SrCO₃

Before preparation of SrTiO₃, calcination of SrCO₃ was required.

SrCO₃ (9.31 g) was weighed on a weighing boat and transferred to an agate mortar. The sample was mortared for 2 min and transferred into a porcelain crucible. The crucible covered with lid was transferred into the Nabertherm Muffle furnace L3/11/P320 (Nabertherm GmbH) and the heating program was started (300 °C, 1 h, heating rate 10 °C/min). After calcination was finished, the sample was removed from the furnace and weighed. The sample was a white powder, m = 9.24 g, yield 99.2%.

3.2. Preparation of SrTiO₃

Freshly calcined SrCO₃ (6.21 g, 42 mmol, 1 equiv.) was weighed in a weighing boat, TiO₂ (3.37 g, 42 mmol, 1 equiv.) was weighed in another weighing boat. The weighed samples were transferred to an agate mortar and mixed for approx. 10 min. During mixing, 250 µL of EtOH was added to the mixture and the mortaring of solid was continued. The procedure of EtOH addition was repeated 3 more times.

After mortaring, the mixture of solids was transferred to a 150 mL alumina crucible. The mixture was pressed with an agate pestle (without applying force, just to make the solid mixture a bit more compact inside the crucible).

The crucible covered with lid was transferred to a Nabertherm LT15/11/P330 (Nabertherm GmbH) muffle furnace and the heating program was started (1000 °C, 1 h, heating rate 10 °C/min). After calcination was finished, the solid from the crucible was transferred to a

weighing bowl and the lumps were broken into smaller pieces with plastic spatula to make the solid more homogeneous. The solid after calcination was represented with white solid, m = 7.64 g, yield = 99.0 %.

3.3. Al doping of SrTiO₃

SrCl₂•6H₂O (79.95 g, 299.86 mmol, 10 equiv.) was weighed in a bowl. SrTiO₃ (5.55 g, 30.246 mmol, 1 equiv.) was weighed in a weighing bowl. The materials were transferred to an agate mortar and the mixture was mortared for approx. 15 min. The mortared solid was distributed between three 150 mL alumina crucibles. The mixture inside the crucible was pressed with an agate pestle (without applying force, just to make the solid mixture a bit more compact inside the crucible).

The crucibles covered with lid was transferred to a Nabertherm LT15/11/P330 (Nabertherm GmbH) muffle furnace and the heating program was started (1000 °C, 10 h, heating rate 10 °/min). After cooling down, the crucibles were removed.

25 mL of water was added to each alumina crucible via a graduated cylinder. The suspension inside the crucible was scratched with plastic spatula, afterwards the suspension was left for 1 h for better dissolution of SrCl₂ and further transfer of the calcined solid from the crucible.

After 1 h, the suspension was sonicated in an ultrasonic bath for 15 s. Next, the suspension was transferred to a 600 mL glass beaker. To remove the total amount of calcined solid, the crucibles were filled with 25 mL water one more time and left for approx. 10-15 min. Afterwards, the samples were sonicated in an ultrasonic bath and transferred to the 600 mL glass beaker. This was repeated 4 more times to transfer the solid from the crucible quantitatively.

Next, the sample was filtered using a PVDF filter (0.22 µm pore diameter). Afterwards, the collected solid on the top of the filter was thoroughly washed with water (70 °C), carefully scratching the slurry to provide thorough washing of the solid. Periodically, Cl⁻ tests with the use of 0.1 M AgNO₃ solution were performed (in total, 16 tests were performed till the solution after mixing with 0.1 M AgNO₃ became clear and overall approx. 10 L of water for washing procedure was used).

The washed solid on the top of the PVDF filter was transferred to a Petri dish by creating a slurry (roughly, approx. 30 mL of water was added to a PVDF filter, the solid was carefully scratched from the surface to create a slurry and transfer it afterwards to a Petri dish using a glass pipette). The Petri dish was covered with Al foil with perforated holes in it. The dish was transferred to a drying oven (100 °C, 12 h). Afterwards, the dried sample was collected from the Petri dish and weighed. The final product (Al:SrTiO₃) was represented with creamy solid, m = 5222.61 mg, yield = 94.1 %.

3.4. $\text{RhCl}_3 \times 3\text{H}_2\text{O}$ and $\text{Cr}(\text{NO}_3)_3 \times 9\text{H}_2\text{O}$ stock solutions preparation

$\text{RhCl}_3 \times 3\text{H}_2\text{O}$ (13 mg, 0.049 mmol) was weighed on a weighing paper and transferred to a 10 mL vial. $\text{Cr}(\text{NO}_3)_3 \times 9\text{H}_2\text{O}$ (57.64 mg, 0.144 mmol) was weighed in a 10 mL vial. Water (2000 μL) was added to each vial to dissolve the solids. The solutions were transferred to a 15 mL Falcon tube. 1000 μL of water was added to each vial to transfer the solution from the vial quantitatively to the Falcon tube. The volume of each solution was adjusted to 5 mL by gradual addition of water till the constant volume.

3.5. Loading of Al:SrTiO₃ with Rh_{2-y}Cr_yO₃ co-catalyst

Al:SrTiO₃ (500.12 mg, 2.725 mmol) was weighed on a weighing paper and transferred to a 100 mL borosilicate 3.3 beaker. Water (12.5 mL) was transferred to the beaker and stirring (300 rpm) was started. $\text{RhCl}_3 \times 3\text{H}_2\text{O}$ solution (492 μL , 9.874 mM) was added fast to the suspension under stirring, afterwards $\text{Cr}(\text{NO}_3)_3 \times 9\text{H}_2\text{O}$ solution (334 μL , 28.809 mM) was added fast to the suspension under stirring. The mixture was stirred for ca. 3 min for better distribution of the components.

The beaker was transferred to a water bath (70 °C). After evaporation of the total amount of water, the stirring and heating was stopped.

The crystallizing dish (borosilicate glass, d = 8 cm) was placed on a beaker as a lid. The beaker covered with lid was transferred to the Nabertherm Muffle furnace L3/11/P320 (Nabertherm GmbH) and the heating program was started (350 °C, 1 h, heating rate 10 °/min). After calcination was finished, the solid from the beaker was collected from the walls and the bottom of the beaker and weighed. The final product was represented with light grey-pinkish solid, m = 495.98 mg, yield = 99.2 %.

For preparation of the photocatalyst with 0.05 wt% Rh and Cr content in the final product the following procedure was applied.

Al:SrTiO₃ (149.51 mg, 0.81 mmol) was weighed on a weighing paper and transferred to a 25 mL borosilicate beaker afterwards. Water (3876 μL) was transferred to the beaker, placed on the magnetic stirrer (Heidolph) and the stirring was started (400 rpm). $\text{RhCl}_3 \times 3\text{H}_2\text{O}$ solution (74 μL , 9.874 mM) was added to the suspension under stirring, afterwards $\text{Cr}(\text{NO}_3)_3 \times 9\text{H}_2\text{O}$ solution (50 μL , 28.809 mM) was added to the suspension under stirring. The mixture was stirred for ca. 3 min for better distribution of the components.

The beaker was transferred to a water bath equipped with an external temperature sensor from the magnetic stirrer, afterwards, the heating was started (70 °C, precise mode). After evaporation of the total amount of water (ca. 2 h), the stirring and heating were stopped. The dried solid was transferred to a quartz crucible using Smartspatula. The quartz crucible covered with lid was placed in Nabertherm muffle furnace L3/11/P320 (Nabertherm GmbH), and the heating program was started (350 °C, 1 h, heating rate 10 °/min). After calcination was finished, the solid from the crucible was weighed. The final product was represented with creamy-greyish solid, m = 142.14 mg, yield = 95.1 %.

For preparation of the photocatalyst with 0.2 wt% Rh and Cr content in the final product the following procedure was applied.

$\text{Al}:\text{SrTiO}_3$ (152.05 mg, 0.83 mmol) was weighed on a weighing paper and transferred to a 25 mL borosilicate beaker afterwards. Water (3505 μL) was transferred to the beaker, placed on the magnetic stirrer (Heidolph) and the stirring was started (400 rpm). $\text{RhCl}_3 \times 3\text{H}_2\text{O}$ solution (295 μL , 9.874 mM) was added to the suspension under stirring, afterwards $\text{Cr}(\text{NO}_3)_3 \times 9\text{H}_2\text{O}$ solution (200 μL , 28.809 mM) was added to the suspension under stirring. The mixture was stirred for ca. 3 min for better distribution of the components.

The beaker was transferred to a water bath (Benmari-crystallizing dish 8cm filled with water) equipped with an external temperature sensor from the magnetic stirrer. The heating was started (70°C , precise mode). After evaporation of the total amount of water (ca. 2 h), the stirring and heating was stopped. The dried solid was transferred to a quartz crucible using Smartspatula. Quartz crucible covered with lid was placed in Nabertherm muffle furnace L3/11/P320 (Nabertherm GmbH). and the heating program was started (350°C , 1 h, heating rate $10^\circ\text{C}/\text{min}$). After calcination was finished, the solid from the crucible was weighed. The final product was represented with creamy-greyish solid, $m = 142.57\text{ mg}$, yield = 93.8 %.

3.6. Photocatalyst characterization

The morphology of the obtained photocatalyst is presented in [Figure 1](#).

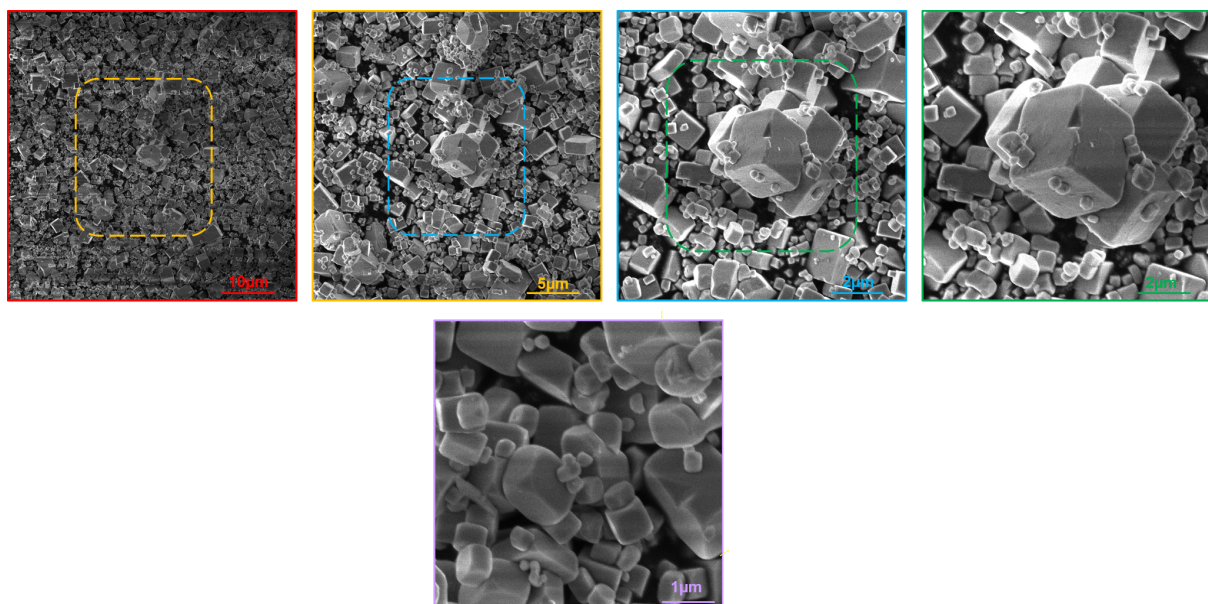


Figure 1: SEM images of $\text{Al}:\text{SrTiO}_3$ loaded with $\text{Rh}_{2-y}\text{Cr}_y\text{O}_3$ co-catalyst at different magnifications

The truncated, cubic-like crystals were formed after Al flux treatment. These crystals with specific facets appear in different sizes. These cube-shaped particles can be seen with edge

sizes between 500 nm to 2 μ m. The majority of the particles were within the 0.5 μ m range, whereas the larger particles appeared partially.

Results of EDX analysis with the spectral distribution of the main elements (O, Sr, Ti, Al, Rh, Cr) of the sample and mapping are presented in [Figure 2](#).

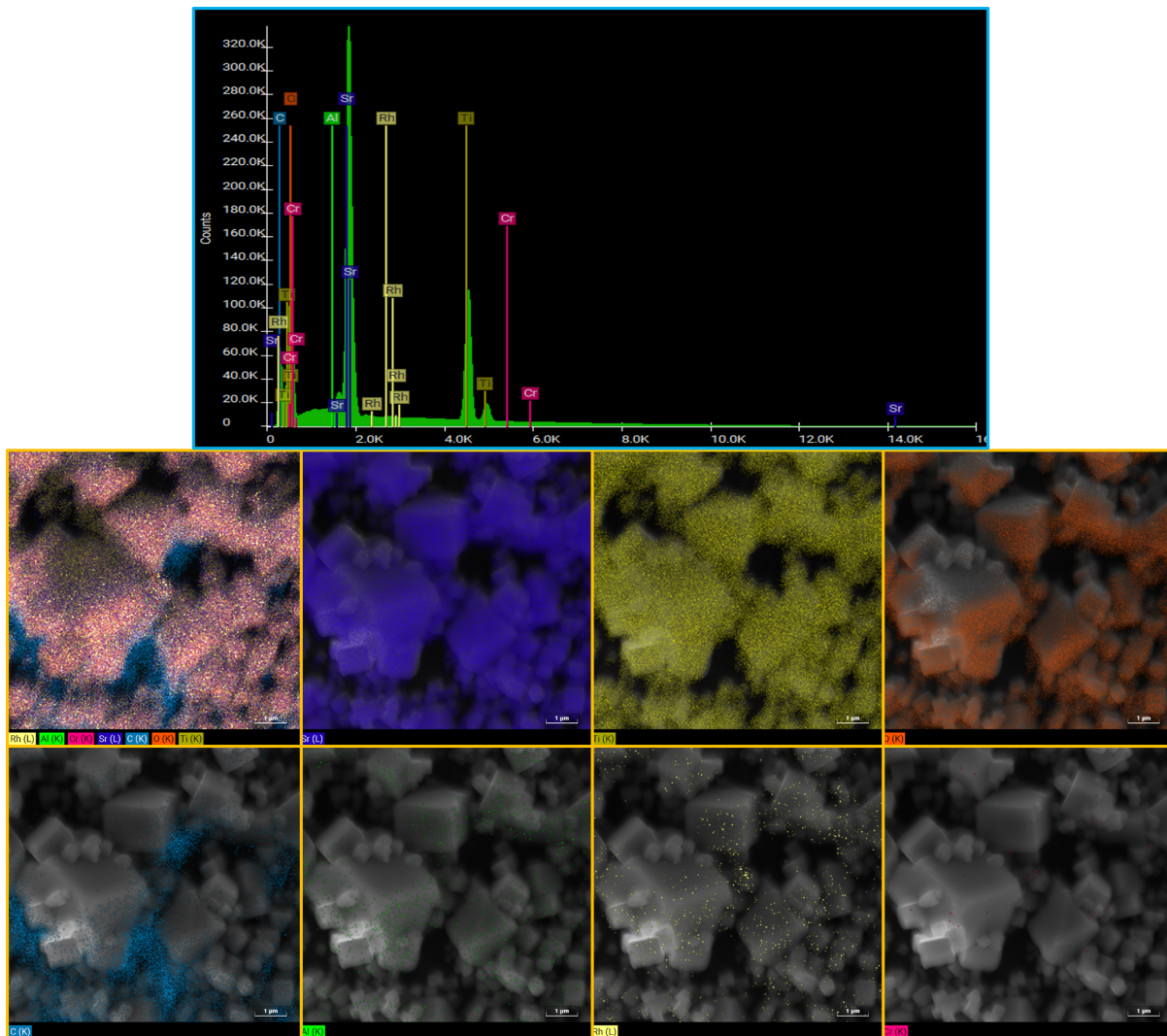


Figure 2: Spectral distribution of the main elements in Al:SrTiO₃ loaded with Rh_{2-y}Cr_yO₃ photocatalyst (top), EDX overview of the sample (bottom)

EDX analysis confirmed the formation of SrTiO₃ as a main phase, the presence of Al in the sample from the doping process and Rh and Cr from the wet impregnation step. The signal of C comes from the conductive carbon tape.

Diffractogramm of the photocatalyst is presented in [Figure 3](#).

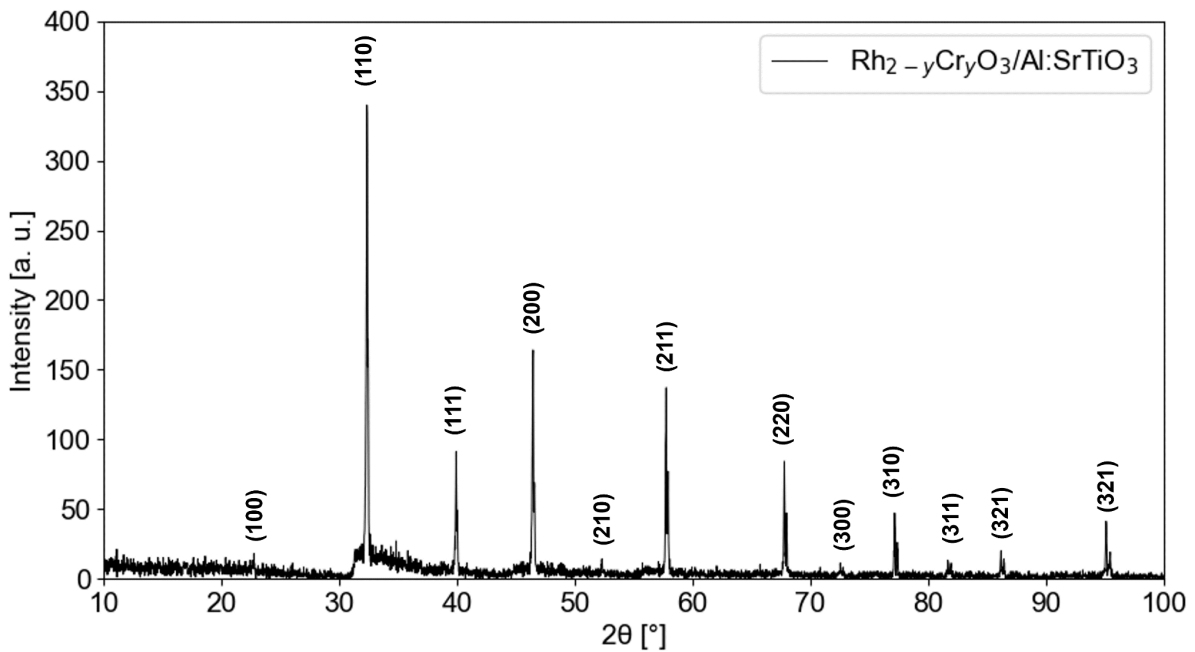


Figure 3: XRD plot of the Al:SrTiO₃ loaded with Rh_{2-y}Cr_yO₃ co-catalyst

The structure is in good agreement with cubic perovskite structure of SrTiO₃ according to JCPDS Card No. 35-0734^[2].

4. Photocatalytic experiment hardware

4.1. Irradiation setup and chamber

The setup consisted of a black, wooden box (L x W x H: 50 x 45 x 70 cm), mounted on black aluminium profiles (40x40 mm, light-duty, slot 8, I-type). A 15 x 15 cm opening (25 cm above the base) was cut into the back wall to allow routing of tubing and cables. Inside the enclosure, two lab jacks and a laboratory stand were installed. The 365 nm LED was placed on one lab jack and a magnetic stirring plate on the other. An irradiation chamber inspired by the design in ^[3] was positioned on the stirring plate (see [Figure 4](#), left).

The chamber was fabricated from polylactic acid using fuse-deposition modelling, employing black filament (Primacreator, Primavalue PLA+ black, 1.75 mm filament size) to minimize light reflection and scattering. The internal dimensions were 130 x 130 x 130 mm. The chamber comprised two side walls with horizontal slots for the reactor holder, as well as an aperture where on one side a solid dummy aperture was installed and on the other side an irradiation aperture. The back wall contained a cutout for water-cooling tubing. In the bottom an aperture for the double-walled beaker was placed (see [Figure 4](#), right).

The double-walled beaker had an inner diameter of approx. 45 mm and an outer diameter of approx. 60 mm, with inner and outer heights of approx. 50 and 60 mm. Opposing inlet (bottom) and outlet (top) were connected to a thermostat (Lauda Loop 100). Both the inner compartment and the interspace between the two walls were filled with Milli-Q water. The

aperture for the double-walled beaker was designed in such a way that the center of the light beam was at the center of the double walled beaker.

The reactor was secured in the double-walled beaker using a holder placed in the uppermost slot of the chamber walls. The distance between the 365 nm LED and the center of the reactor was 80 mm.

All CAD drawings and STL files of the irradiation chamber, as well as the assembly description and a sketch of the double walled beaker are available in the referenced GitHub repository and as a stable release on Zenodo.

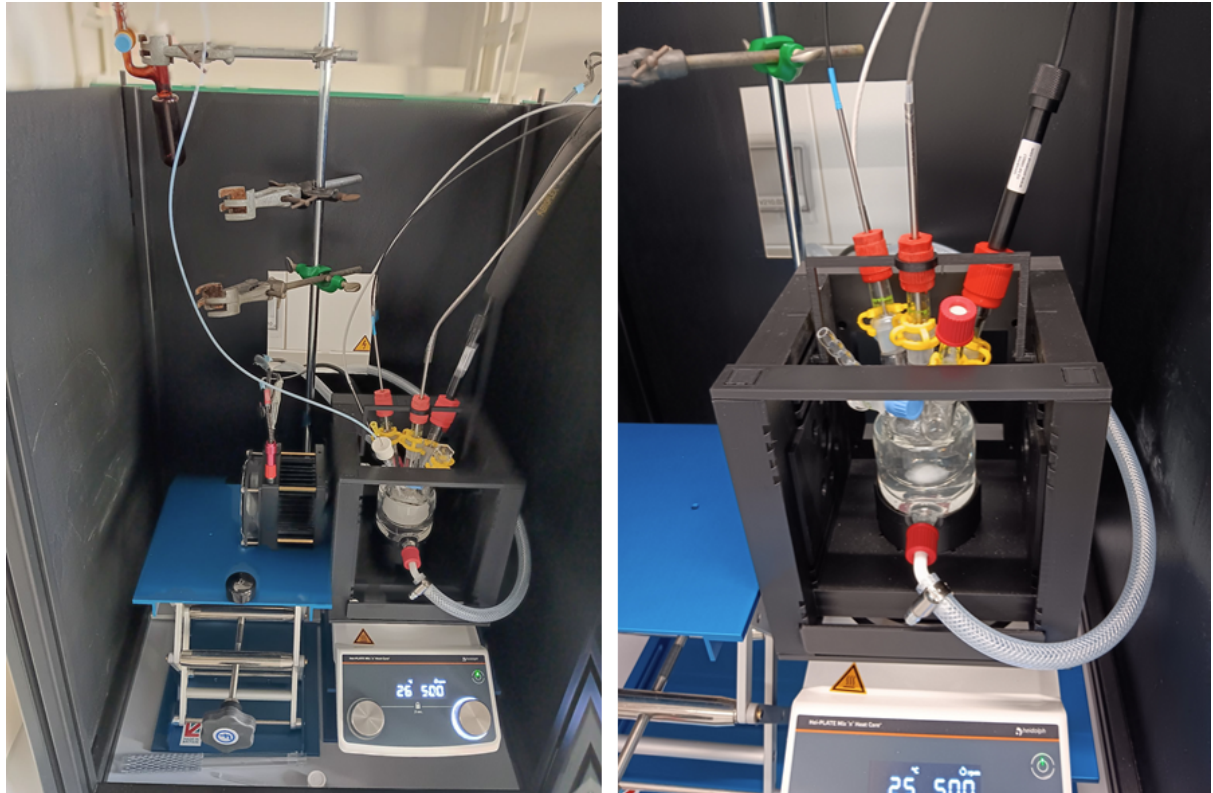


Figure 4: Irradiation setup with installed reactor and sensors. Left: complete irradiation setup, right: close-up of the irradiation chamber

4.2. Irradiation reactor

The reactor was custom built by a glassblower. The main body (see [Figure 5](#)) had a rounded bottom with an outer diameter of 40 mm and a height of approx. 40 mm up to the beginning of the necks. Five outlets were fused onto the top in a cross-shaped arrangement. One outlet contained a valve connection (NS14.5 with a 4 mm bore). The remaining four outlets were NS14 outer joints. For three of these, the total height from the lowest attachment point to the top was approx. 60 mm; the fourth — positioned opposite the valve — was shorter (< 50 mm, see Figure 5).

Each NS14 joint was equipped with a GL14 or GL18 transition adapter. The total adapter height was approx. 60 mm for GL14 and < 50 mm for GL18.



Figure 5: Reactor used for irradiation experiments. Left: Side view with shorter NS14 outlet in front, right: rotated view

4.3. Irradiance determination chamber

Irradiance was measured in a dedicated irradiation chamber similar to the one described in [4.1](#), but modified as follows:

- Solid back wall without cutout
- Solid front wall
- Removable lid on top

These modifications ensured minimal light leakage and allowed the use independently of the full setup.

For irradiance measurements, the power sensor was positioned in the center of the lightbeam using either a holder, inserted into the lowest wall slot or an aperture which was placed into the bottom.

All CAD drawings and STL files of the irradiance determination chamber, as well as the assembly description are available in the referenced GitHub repository and as a stable release on Zenodo.

4.4. Experimental setup for measurements in liquid and gas phase

Summary of the devices used in photocatalytic tests is provided in table 3 below.

Table 3. List of the equipment used in the photocatalytic tests for O₂ and H₂ measurements in liquid and gas phase

Name of the step	Name of the device
Measurements of optical power output	Super high-power 365 nm LED collimator source with a 22 mm clear aperture (LCS-6500-65-22, Mightex Systems) (365 nm LED)
	Newport 843-R-USB power meter (Newport)
	Newport 919P-020-12 thermopile sensor (Newport)
O ₂ measurements (liquid and gas phase)	FireStingO2 optical oxygen meter (FSO2-C2, PyroScience GmbH)
	Trace range robust probe (OXROB10, PyroScience GmbH) in combination with 3 mm BOLA fitting and GL14/NS14 adapter
	PT100 temperature sensor (Therma Thermofühler GmbH) in combination with 4 mm BOLA fitting and GL14/NS14 adapter
H ₂ measurement (liquid phase)	H ₂ UniAmp Single Channel system (Unisense)
	Normal range hydrogen sensor (H ₂ UniAmp Sensor - Normal range - 2.1 x 80 mm needle, Unisense) in combination with 10 mm BOLA fitting and GL18/NS14 adapter
	PT1000 temperature sensor (Therma Thermofühler GmbH) in combination with 4 mm BOLA fitting and GL14/NS14 adapter

	H ₂ UniAmp Single Channel system (Unisense)
H ₂ measurements (gas phase)	Normal range hydrogen sensor (H ₂ UniAmp Sensor - Normal range - 2.1 x 80 mm needle, Unisense) in combination with 2 mm BOLA fitting and GL14/NS14 adapter
	PT1000 temperature sensor (Therma Thermofühler GmbH) in combination with 4 mm BOLA fitting and GL14/NS14 adapter

Photochemical irradiations were performed using the 365 nm LED (For the emission spectrum, see chapter [7.1](#)).

Before each experiment series, the irradiance was measured using the irradiance determination chamber (see section [4.3](#)). Measurements were repeated approx. weekly to account for minor fluctuations in the LED output. The hydrogen sensor was calibrated daily by bubbling hydrogen gas through the solution, as its sensitivity changes over time.

The sensors were installed using gas-tight BOLA laboratory joints. The PT1000 was placed centrally using a 4 mm BOLA joint, after which the reactor was secured in its holder. The PT100 and the FireSting robust probe were installed using 4 and 3 mm BOLA joints, respectively.

5. Photocatalytic experiments with O₂ and H₂ simultaneous detection

5.1. Photocatalyst suspension preparation

In each photocatalytic test, the suspension with photocatalyst concentration 0.5 mg·mL⁻¹ was prepared. Al:SrTiO₃ loaded with Rh_{2-y}Cr_yO₃ (12.5 mg) was weighed in a 50 mL vial followed by addition of H₂O (25 mL) (or D₂O). Next, the suspension was shaken on a vortex mixer for 3 min for homogeneous distribution of photocatalyst particles in the volume of the suspension. Afterwards, the vial was covered with Al foil before further use.

5.2. Main steps in photocatalytic tests

For each experiment, the reactor was placed in the double-walled beaker, the thermostat was set to the desired temperature, and filled with water for the H₂ sensor calibration procedure.

Next, the reactor was deassembled, degreased, washed with fresh portions of water and dried with acetone and compressed air.

Afterwards, the LED was attached to the irradiation chamber. The reactor was assembled again, PTFE stirring bar and the prepared photocatalyst suspension (25 mL, described in [chapter 5.1](#)) was transferred to the reactor using glass pipette followed by the addition of three sensors (O_2 sensor, PT100 and PT1000 sensors), sensor heights were adjusted, when needed, to be comparable. Degassing was performed for approx. 30 min using argon sparging with a PTFE cannula inserted *via* the valve outlet. Afterwards, the Unisense hydrogen sensor was introduced under argon counterstream. The needle tip was oriented toward the LED.

The main steps of the photocatalytic test are presented in [Figure 6](#).

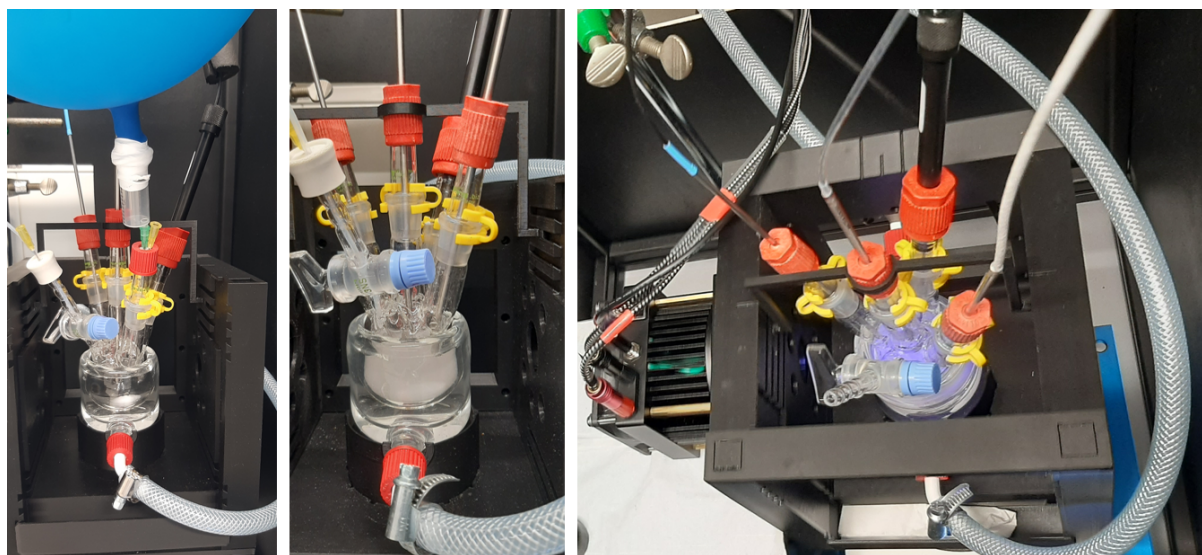


Figure 6: Important steps during photocatalytic tests: calibration of H_2 sensor under degassed conditions (left), degassing of the photocatalyst suspension (center), after start of irradiation, top view (right)

After sensor installation, the PTFE cannula was removed and the reactor was closed. A pre-reaction baseline was recorded for 10 min, followed by irradiation for 15 min and a post-reaction baseline for 10 min.

6. Overview of performed photocatalytic tests

Summary of the experimental conditions used in experiments is provided in [table 4](#) below.

Table 4. Overview of main screening parameters

Parameters	Values
Irradiance, $mW \cdot cm^{-2}$	20, 50, 100, 150
Temperature	10, 20, 30
Co-catalyst loading (Rh, Cr content, wt%)	0.05, 0.1, 0.2

Catalyst concentration, mg·mL ⁻¹	0.5
Dispersion medium	H ₂ O, D ₂ O

Groups of photocatalytic tests according to the varied conditions (irradiance, temperature, co-catalyst loading, dispersion medium, measurements in gas phase) were classified in the following manner (according to [table 5](#)) (for feasibility, the varied values in each group are highlighted with bold).

Table 5. Classification of performed photocatalytic tests

Group name [a]	Irradiance, mW·cm ⁻²	Temperature, °C	Co-catalyst loading, Rh,Cr wt%	D ₂ O	Experiment number
Reference	50	20	0.1	No	NB-316, NB-319, NB-320, NB-329, NB-331, NB-336, NB-339, NB-348, NB-353, NB-356
Irradiance	20	20	0.1	No	NB-325, NB-326, NB-337, NB-345
	100	20	0.1	No	NB-318, NB-322
	150	20	0.1	No	NB-344, NB-347
Temperature	50	10	0.1	No	NB-351, NB-359, NB-360
	50	30	0.1	No	NB-330, NB-334
Loading	50	20	0.05	No	NB-327, NB-332, NB-354, NB-357
	50	20	0.2	No	NB-328

					NB-333, NB-355, NB-358
D ₂ O	50	20	0.1	Yes	NB-346, NB-349
Gas phase	50	20	0.1	No	NB-312, NB-361, NB-362, NB-363, NB-364
Gas phase D ₂ O	50	20	0.1	Yes	NB-365, NB-366, NB-367

^[a] General reaction conditions: 25 mL H₂O, 0.5 mg (catalyst)·mL⁻¹, 365 nm LED irradiation, 10 min pre-reaction baseline, 15 min irradiation, 10 min post-reaction baseline

7. Analytical data

7.1. Spectrum of light source

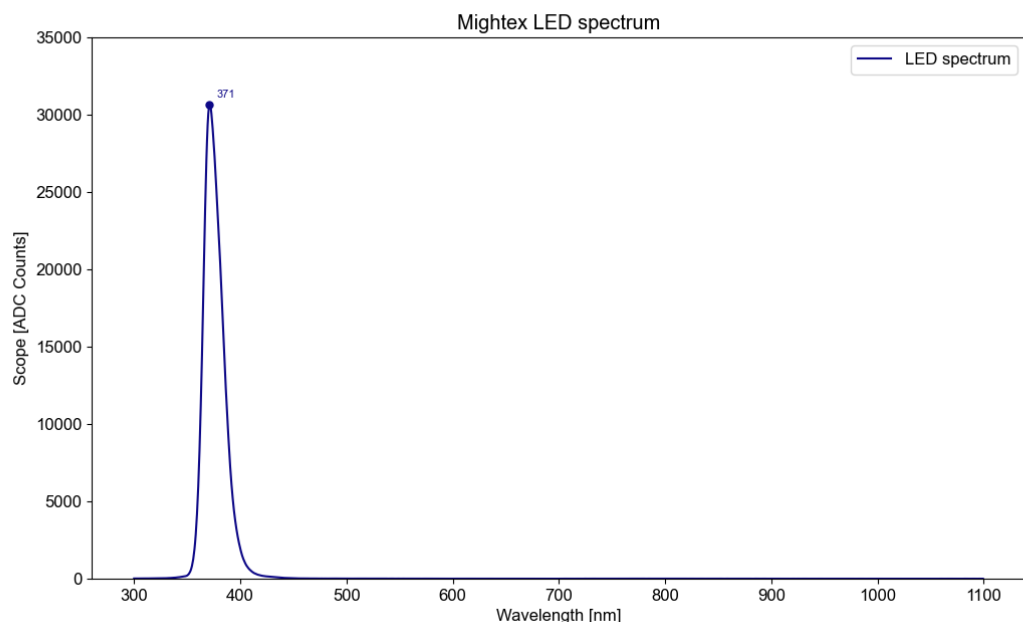


Figure 7: Emission spectrum of 365 nm LED.

8. Data processing and analysis

The entire code (Python) for data analysis and processing and analysis is open-source and can be found in the GitHub repository provided on the title page.

8.1. Detailed description of data processing workflow

From the raw experimental data the reaction phase is selected by selecting the interval between the start and end point of irradiation. Furthermore, the first 60 s after the start of irradiation are removed due to diffusion of gases into the sensors causing an induction period.

The data is then shifted on the x-axis so that the start of irradiation is at $t = 0$ s. Furthermore, the data is shifted on the y-axis so that the initial concentration is equal to $0 \text{ }\mu\text{mol}\cdot\text{L}^{-1}$.

For gas phase data, the raw data (which is in the unit Pa for H_2 and vol% for O_2) is converted to μmol based on the volume of the gas phase, normal atmospheric pressure (101.325 Pa) and the ideal gas law. Furthermore, the amount of gases in μmol is scaled to the amount of gas that would be produced by one liter of liquid phase (using the experimental liquid phase volume), to obtain the unit $\mu\text{mol}\cdot\text{L}^{-1}$ (for consistent units across liquid and gas phase).

To the thus obtained reaction data, a polynomial is fitted (4th order polynomial for liquid phase data, 3rd order polynomial for gas phase data). Furthermore, the experimental data is smoothed using a Savitzky-Golay filter (for H_2 : window size: 30, polynomial order: 1; for O_2 : window size: 10, polynomial order: 3). Both the fitted polynomial and the smoothed data are numerically differentiated to obtain the corresponding rate data. The maximum of the differentiated polynomial is picked to obtain the maximum rate.

8.2. Liquid/gas phase mass transport during photocatalytic water splitting

Using the photocatalytic reactor set-up and prepared photocatalyst, we initially wanted to investigate the mass transport of H_2 and O_2 from the liquid into the gas phase during photocatalytic water splitting. We performed two sets of experiments, where we detected H_2/O_2 once in the liquid and once in the gas phase, measuring the evolution of both gases over time.

In the liquid phase, immediate formation of both H_2 and O_2 can be observed (see [Figure 8](#)), although the rate is slightly slower at the beginning. In the gas phase, a pronounced induction period of around three minutes is observed due to diffusion of the gases from the liquid to the gas phase. Experimentally, it can be seen that the ratio of H_2 and O_2 is not constant over time: in the liquid phase, it starts at ca. 2:1 H_2/O_2 but quickly decreases to a ratio of 1.4:1. In the gas phase, the initial ratio is around 2.5:1 and gradually decreases to 2:1.

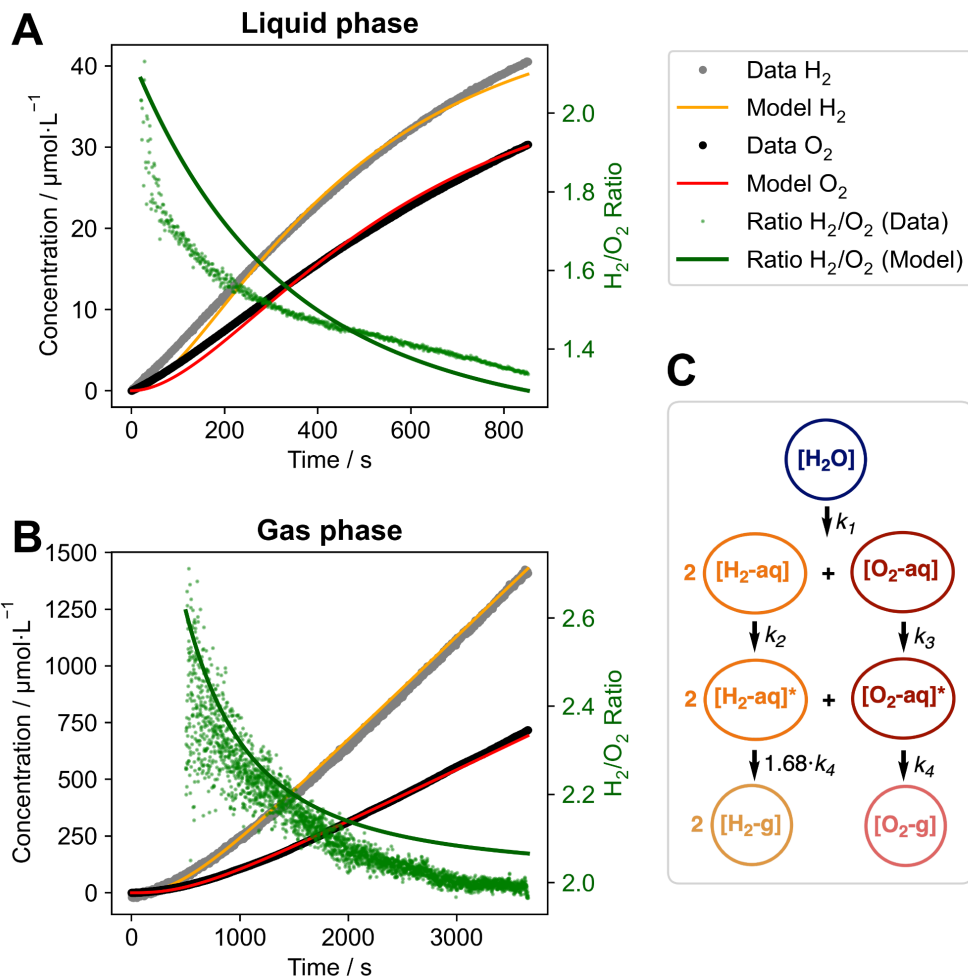


Figure 8: Experimental data and kinetic modelling of H₂/O₂ evolution in the liquid (**A**) and gas phase (**B**). For both measurements the evolution of the gases over time is shown (black and grey dots) as well as the ratio between the two gases (right axis, green dots). The concentration of the liquid phase gases is given in $\mu\text{mol}\cdot\text{L}^{-1}$ and the gas phase concentration is given in an analogous unit of $\mu\text{mol}\cdot\text{L}^{-1}$, which indicates the amount of gases formed per liter of irradiated liquid phase volume (to have consistent units for the kinetic modelling). To both the liquid and the gas phase data one kinetic model (**C**) with one set of rate constants is fitted (black, grey and green lines). The optimized values for the rate constants are: $k_1 = 4.1 \cdot 10^{-9} \text{ s}^{-1}$, $k_2 = 2.3 \cdot 10^{-3} \text{ s}^{-1}$, $k_3 = 2.2 \cdot 10^{-3} \text{ s}^{-1}$, $k_4 = 5.8 \cdot 10^{-3}$.

To rationalize these observations, we fitted to the data a simple kinetic model (see [Figure 8C](#)). This model is deliberately chosen to be as simple as possible and is only intended to provide a phenomenological description of the experimental observations.

The model is composed of the following reaction steps:

- Step 1: $[\text{H}_2\text{O}] > 2[\text{H}_2\text{-aq}] + [\text{O}_2\text{-aq}], k_1$
- Step 2: $[\text{H}_2\text{-aq}] > [\text{H}_2\text{-aq}]^*, k_2$
- Step 3: $[\text{O}_2\text{-aq}] > [\text{O}_2\text{-aq}]^*, k_3$
- Step 4: $[\text{O}_2\text{-aq}]^* > [\text{O}_2\text{-g}], k_4$
- Step 5: $[\text{H}_2\text{-aq}]^* > [\text{H}_2\text{-g}], k_4 \cdot 1.68$

Step 1 described the water splitting reaction forming two equivalents of H₂ and one equivalent of O₂. Steps 2 and 3 describe the diffusion of H₂ and O₂ within the liquid phase, respectively, especially to reach the sensors. Steps 4 and 5 describe the diffusion of both gases from the liquid to the gas phase. Here, the same rate constant (k_4) is used for both cases, but for H₂ it is multiplied by a factor of 1.68, which is the ratio between the solubilities/Henry's constants of the two gases.

Fitting this model simultaneously to the H₂ and O₂ data in the liquid and gas phase (with just one set of values for the rate constants, using a differential evolution algorithm) gives acceptable agreement with both the time evolution of the gases as well as the observed ratios over time (see [Figure 8](#)).

The evolution of the H₂/O₂ ratios over time can be understood based on the different solubilities of H₂ and O₂ in water (as described by the ratio of the Henry's law constants): due to the lower solubility of H₂, it diffuses out of the liquid phase more quickly, leading to a lower H₂/O₂ ratio in the liquid phase (converging to roughly 1.2:1) and correspondingly a higher initial H₂/O₂ ratio in the gas phase. In the gas phase, the H₂/O₂ ratio does converge to the expected 2:1 ratio over time.

It should be stated clearly that this simplified model is purely phenomenological and is only intended to provide a qualitative understanding for the reason why the H₂/O₂ ratios in the liquid and gas phase evolve over time.

8.3. Processed experimental data

Liquid phase data:

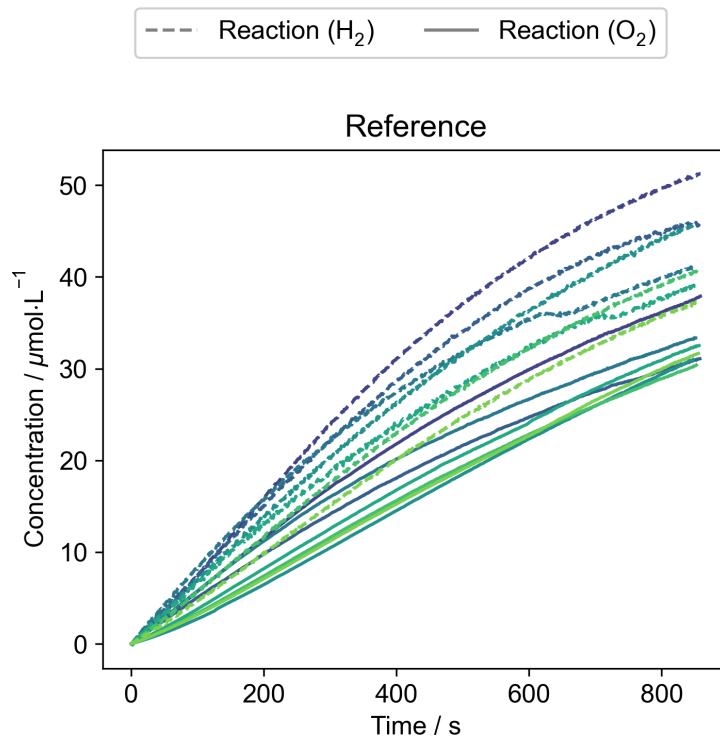


Figure 9: Experimental data for H₂/O₂ simultaneous measurements (reference conditions)

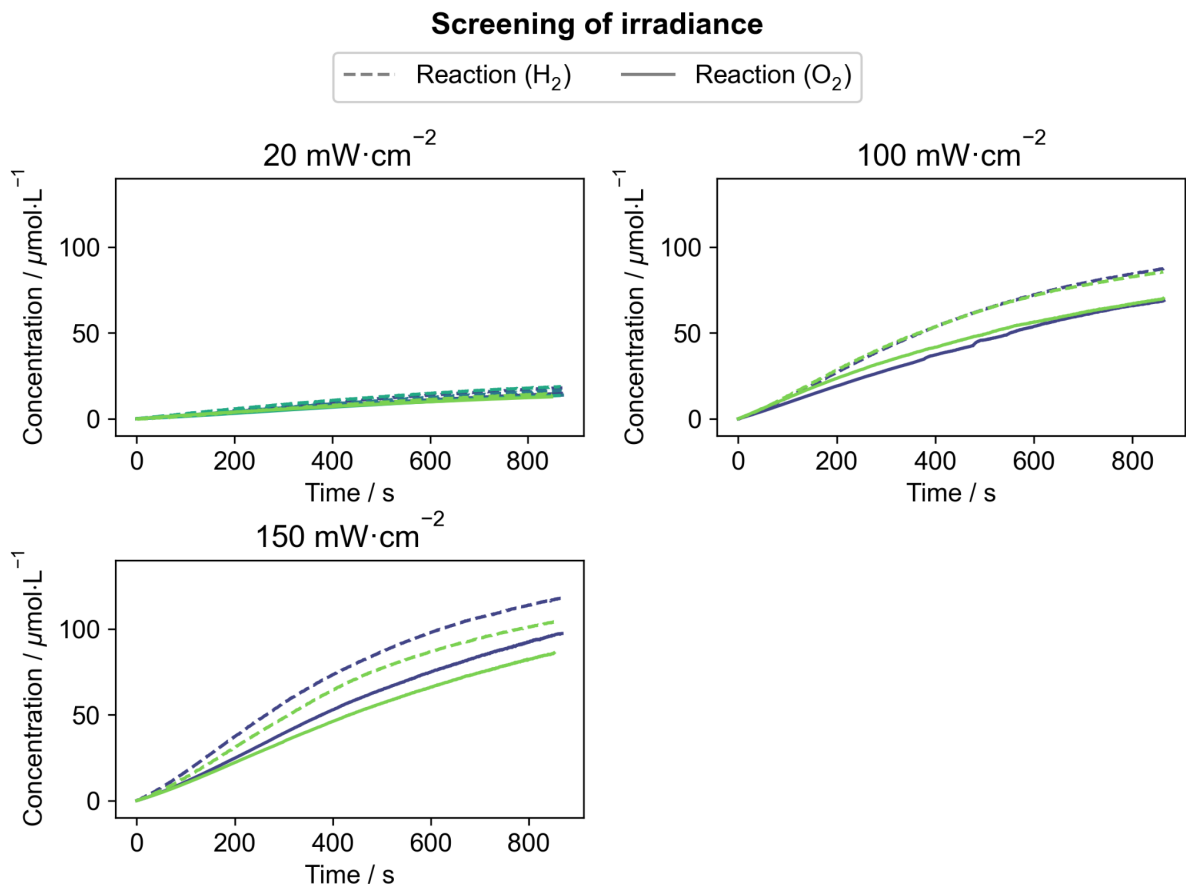


Figure 10: Experimental data for H_2/O_2 simultaneous measurements (screening of irradiance: $20 \text{ mW}\cdot\text{cm}^{-2}$, $100 \text{ mW}\cdot\text{cm}^{-2}$, $150 \text{ mW}\cdot\text{cm}^{-2}$)

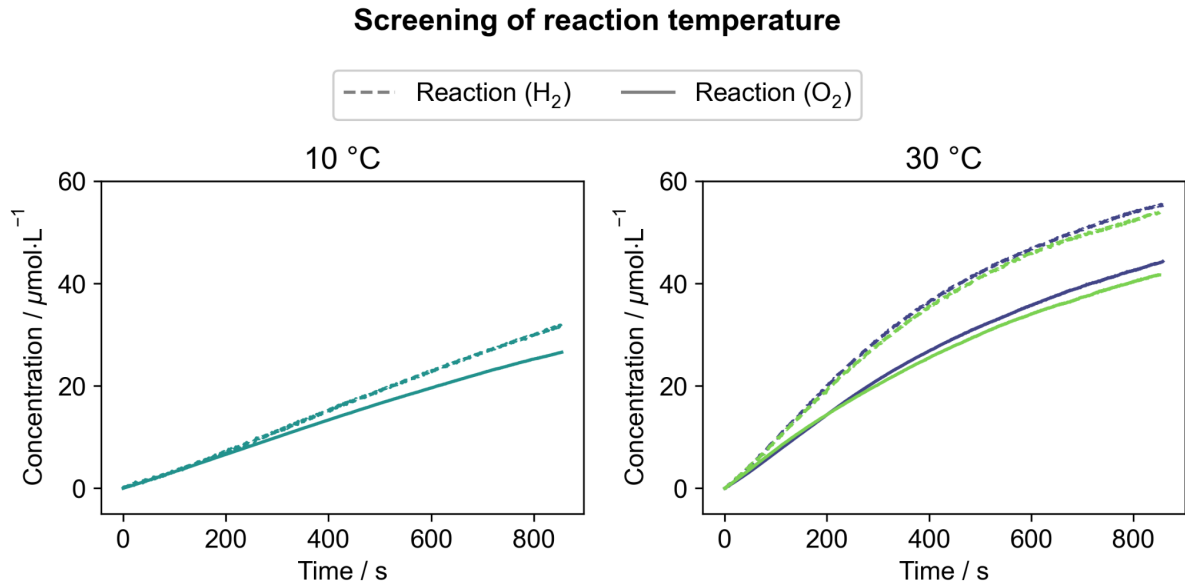


Figure 11: Experimental data for H_2/O_2 simultaneous measurements (screening of temperature: $10 \text{ }^\circ\text{C}$, $30 \text{ }^\circ\text{C}$)

Screening of co-catalyst loading

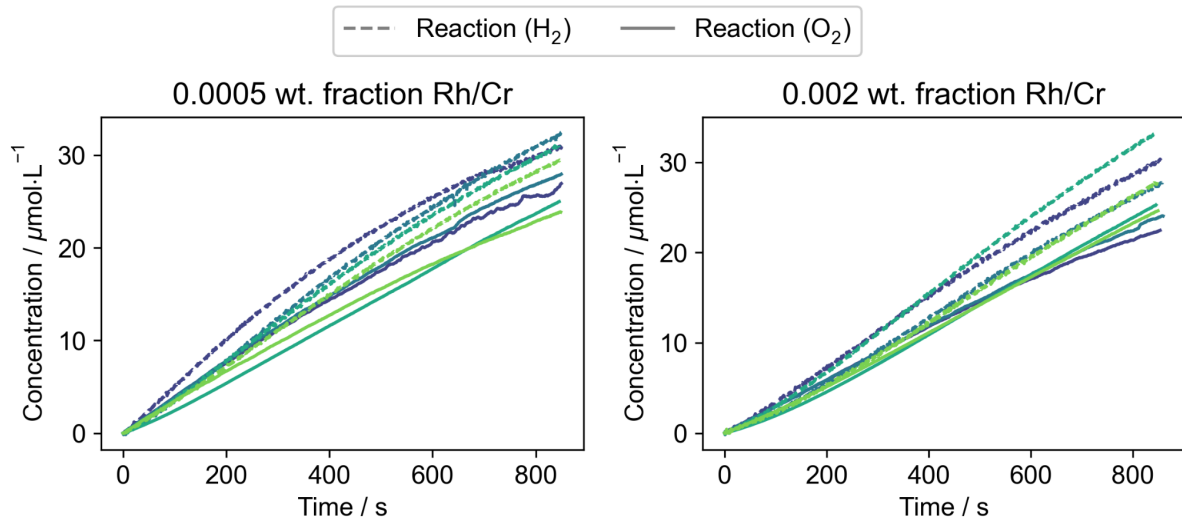


Figure 12: Experimental data for H₂/O₂ simultaneous measurements (screening of co-catalyst loading: 0.0005 wt. fraction Rh/Cr, 0.002 wt. fraction Rh/Cr)

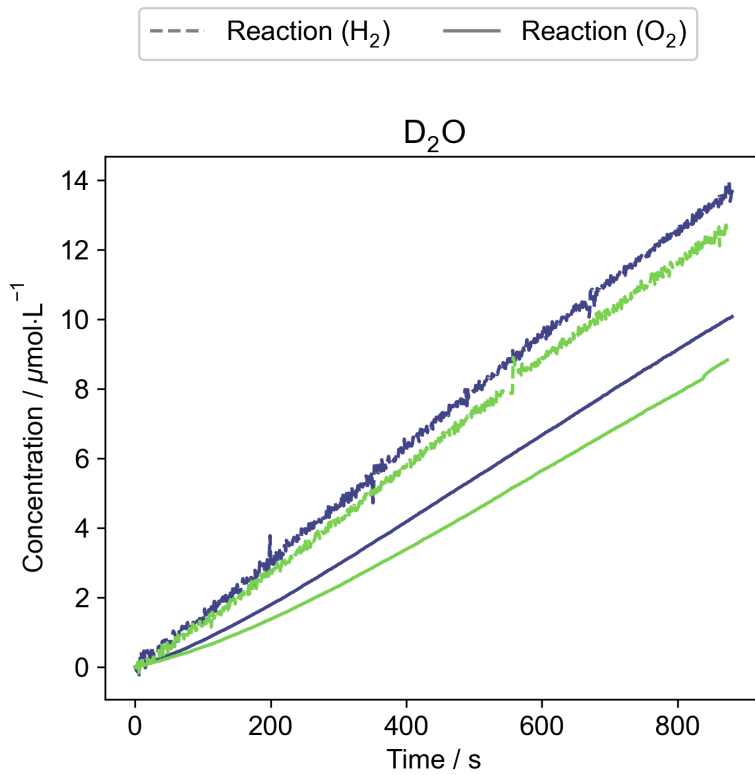


Figure 13: Experimental data for H₂/O₂ simultaneous measurements (kinetic isotope effect investigation)

Gas phase data:

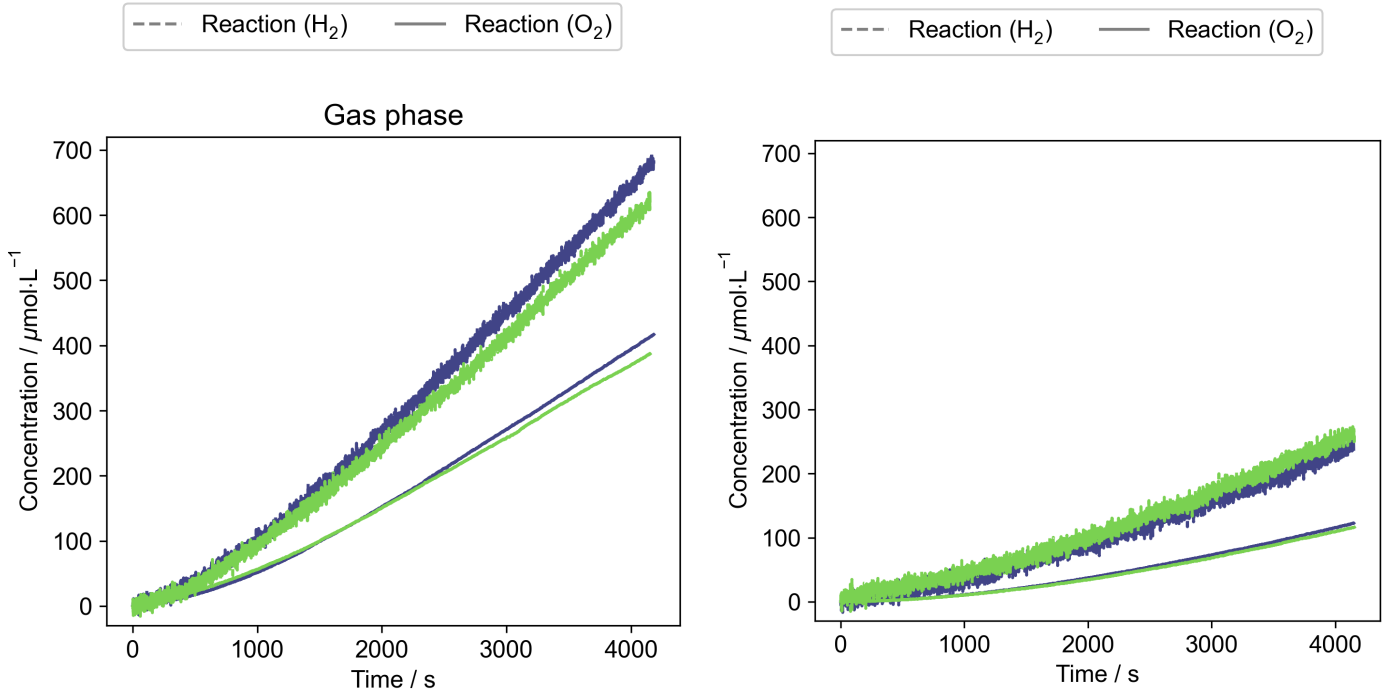


Figure 14: Experimental data for H₂/O₂ simultaneous measurements in gas phase (left: H₂O as a dispersion medium, right: D₂O as a dispersion medium for kinetic isotope effect investigation)

8.4. Arrhenius analysis of temperature dependent data

The temperature-dependent liquid phase data was analyzed based on Arrhenius' equation, through standard logarithmic linearization, followed by linear regression to determine the activation energy based on both the H₂ and O₂ data:

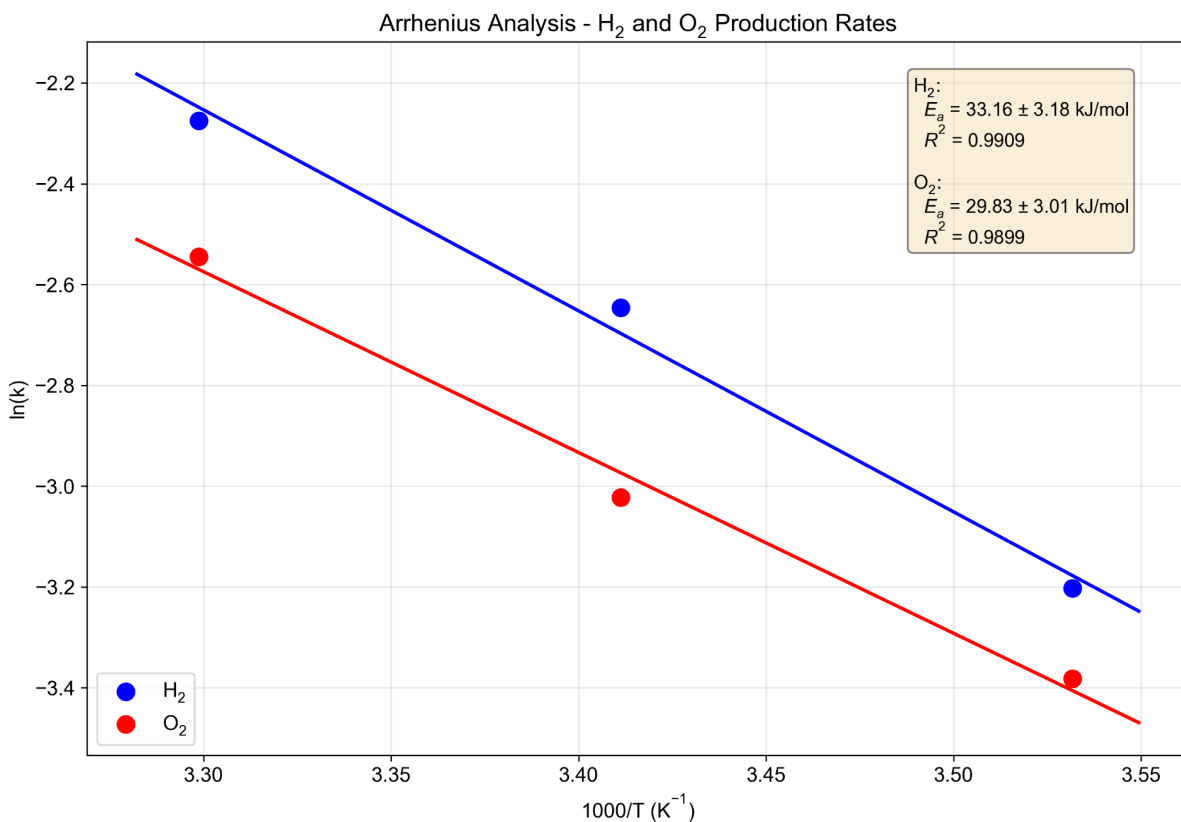


Figure 15: Arrhenius analysis of temperature dependent liquid phase experimental data to determine the thermal activation energy

9. References

1. Z. Zhao, R. V. Goncalves, S. K. Barman, E. J. Willard, E. Byle, R. Perry, Z. Wu, M. N. Huda, A. J. Moulé, F. E. Osterloh, *Energy Environ. Sci.* **2019**, *12*, 1385-1395.
2. JCPDS-International Centre for Diffraction Data, Card No. 35-0734.
3. D. Kowalczyk, P. Li, A. Abbas, J. Eichhorn, P. Buday, M. Heiland, A. Pannwitz, F. H. Schacher, W. Weigand, C. Streb, D. Ziegenbalg, *ChemPhotoChem.* **2022**, *6* (7), e202200044.